Solution structure of the extended neuronal nitric oxide synthase PDZ domain complexed with an associated peptide

Hidehito Tochio, Qiang Zhang, Pravat Mandal, Ming Li and Mingjie Zhang

Department of Biochemistry, The Hong Kong University of Science and Technology, Clear Water Bay, Kowloon, Hong Kong, P. R. China

The PDZ domain of neuronal nitric oxide synthase (nNOS) functions as a scaffold for organizing the signal transduction complex of the enzyme. The NMR structure of a complex composed of the nNOS PDZ domain and an associated peptide suggests that a two-stranded β-sheet C-terminal to the canonical PDZ domain may mediate its interaction with the PDZ domains of postsynaptic density-95 and α-syntrophin. The structure also provides the molecular basis of recognition of Asp–X–Val-COOH peptides by the nNOS PDZ domain. The role of the C-terminal extension in Asp-X-Val-COOH peptide binding is investigated. Additionally, NMR studies further show that the Asp-X-Val-COOH peptide and a C-terminal peptide from a novel cytosolic protein named CAPON bind to the same pocket of the nNOS PDZ domain.

PDZ domains were originally identified as repeats of ~90 amino acid residues in postsynaptic density-95 (PSD-95), and were named after PSD-95; *Drosophila* discs large tumor suppressor, Dlg; and the mammalian tight junction protein, ZO-1[1–4]. Amino acid sequence analysis showed that PDZ domains are found in a wide array of proteins possessing diverse biological functions[1]. Numerous studies have indicated that PDZ domains are multifunctional protein–protein interaction modules that play important roles in clustering membrane proteins, organizing signal transduction complexes, and maintaining cell polarity[1–6]. One common mode for the interaction of PDZ domains involves association with short peptide fragments at the very C-terminus of target proteins[7,8]. Additionally, PDZ domains have been shown to form hetero-dimers[9–11], and to interact with internal peptide fragments of target proteins[12,13]. Recent structural studies have demonstrated that PDZ domains from various proteins adopt similar three dimensional conformations[7,14–16]. The C-terminal peptides bind to a groove formed by the principal α-helix (αB) and the second β-strand (βB) of the PDZ domains in an anti-parallel fashion (Fig. 1*c*).

Neuronal nitric oxide levels are largely regulated by neuronal nitric oxide synthase (nNOS). nNOS differs from the two other NOS isoforms (endothelial NOS and inducible NOS) in having an ~250 residue N-terminal extension which contains a PDZ domain and a dynein light chain/protein inhibitor (PIN)-binding domain[17–19]. The nNOS PDZ domain targets the enzyme to the cell membrane by binding to PSD-95 and α-syntrophin[3,9]. In addition to its binding to short C-terminal peptides with a Asp/Glu-X-Val* (where '*' denotes the carboxylate of the peptide) sequence[10,11], the nNOS PDZ domain, uniquely, forms heterodimers with the PDZ domain of α-syntrophin and PSD-95[9]. Formation of the above PDZ dimers requires the additional ~25 amino acid residues C-terminal to the canonical nNOS PDZ domain[9,10]. Very recently, a novel cytosolic protein named CAPON was isolated, and the protein was found to bind to nNOS and thereby regulate the interaction of nNOS with PSD-95[20]. CAPON interacts with the nNOS PDZ domain through its C-terminus, even though it does not contain an Asp/Glu-X-Val* motif.

Here, we present the solution structure of the nNOS PDZ domain complexed with a seven-residue target peptide. The three-dimensional structure of the complex provides insights into the structural mechanism of the heterodimer formation

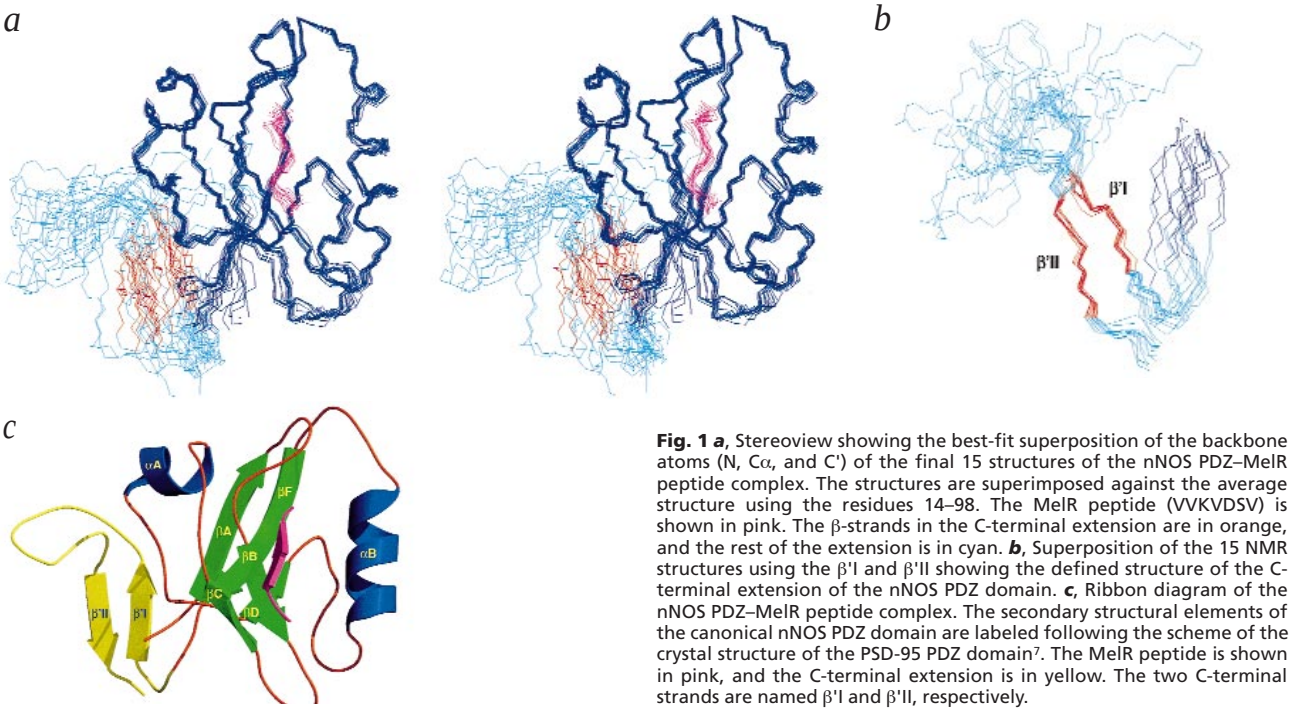

Fig. 1 ***a***, Stereoview showing the best-fit superposition of the backbone atoms (N, Cα, and C') of the final 15 structures of the nNOS PDZ–MelR peptide complex. The structures are superimposed against the average structure using the residues 14–98. The MelR peptide (VVKVDSV) is shown in pink. The β-strands in the C-terminal extension are in orange, and the rest of the extension is in cyan. ***b***, Superposition of the 15 NMR structures using the β'I and β'II showing the defined structure of the C-terminal extension of the nNOS PDZ domain. ***c***, Ribbon diagram of the nNOS PDZ–MelR peptide complex. The secondary structural elements of the canonical nNOS PDZ domain are labeled following the scheme of the crystal structure of the PSD-95 PDZ domain[7]. The MelR peptide is shown in pink, and the C-terminal extension is in yellow. The two C-terminal strands are named β'I and β'II, respectively.

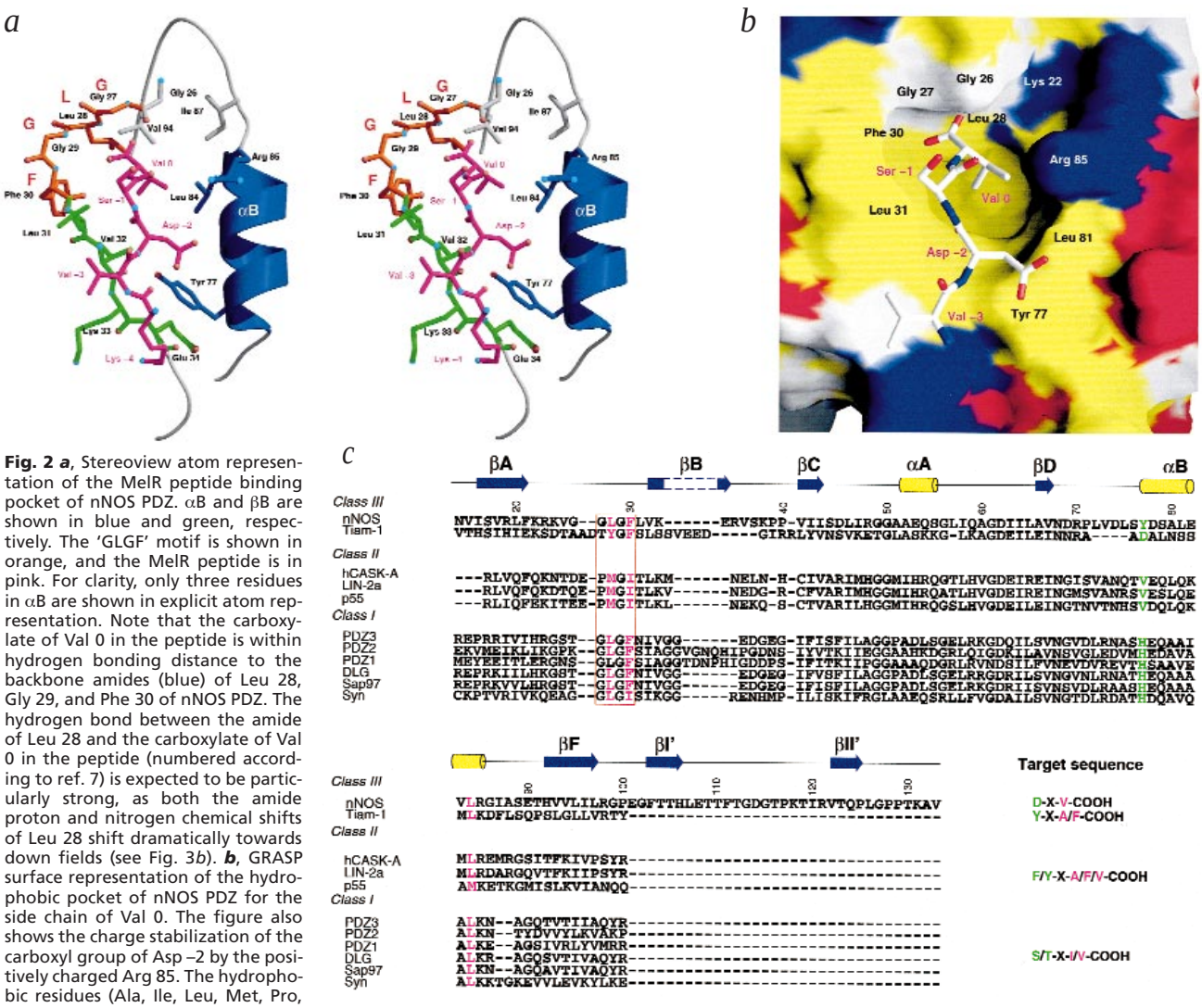

Fig. 2 ***a***, Stereoview atom representation of the MelR peptide binding pocket of nNOS PDZ. αB and βB are shown in blue and green, respectively. The 'GLGF' motif is shown in orange, and the MelR peptide is in pink. For clarity, only three residues in αB are shown in explicit atom representation. Note that the carboxylate of Val 0 in the peptide is within hydrogen bonding distance to the backbone amides (blue) of Leu 28, Gly 29, and Phe 30 of nNOS PDZ. The hydrogen bond between the amide of Leu 28 and the carboxylate of Val 0 in the peptide (numbered according to ref. 7) is expected to be particularly strong, as both the amide proton and nitrogen chemical shifts of Leu 28 shift dramatically towards down fields (see Fig. 3*b*). ***b***, GRASP surface representation of the hydrophobic pocket of nNOS PDZ for the side chain of Val 0. The figure also shows the charge stabilization of the carboxyl group of Asp –2 by the positively charged Arg 85. The hydrophobic residues (Ala, Ile, Leu, Met, Pro, Phe, Tyr, and Val) are shown in yellow, negatively charged residues (Asp and Glu) in red, positively charged residues (Arg, His, and Lys) in blue, and polar residues (Asn, Gln, Gly, Ser, and Thr) in white. ***c***, Amino acid sequence alignment of selected PDZ domains. The secondary structure of nNOS PDZ determined from this work is also included at the top of the sequence. The PDZ domains are divided into class I, II, and III based on their target binding specificity. The 'GLGF' motif is highlighted with an open box. The amino acid residues forming the hydrophobic pocket accommodating the side chain of the residue at position 0 of target peptides are drawn in red, and the amino acid residues that play critical roles in selecting the residue at the –2 position of peptide are in green. The target peptide sequences for each class of PDZ are also included in the figure.

between the nNOS PDZ domain and the PDZ domains of PSD-95 or α-syntrophin. The structure also reveals the target peptide recognition mechanism by the nNOS PDZ domain. The contribution of the C-terminal extension to the target recognition by the nNOS PDZ domain was studied. We have also compared the interactions of the nNOS PDZ domain with: (i) the Asp/Glu-X-Val* peptide and (ii) a synthetic peptide derived from the C-terminus of CAPON.

Structure determination

The three-dimensional structure of the nNOS PDZ domain complexed with a seven-residue synthetic peptide (Val-Val-Lys-Val-Asp-Ser-Val) was solved using a total of 1,734 experimental restraints derived from NMR spectroscopy (Table 1). The nNOS PDZ domain used in this work encompasses amino acid residues 11–133 of the rat enzyme. The amino acid residues outside the canonical PDZ domain (residues 100–133) were shown to be required for nNOS PDZ to interact with the PDZ domain of PSD-95 and α-syntrophin[9,10], and the construct is thus termed the long nNOS PDZ domain (abbreviated here as 'nNOS PDZ'). The seven residue synthetic peptide corresponds to an identical sequence in the C-terminal domain of the melatonin receptor *a* (referred to as the MelR peptide). It has been shown that nitric oxide signaling can be regulated by melatonin[21]. In addition, the Asp-X-Val* motif at the C-terminus of the melatonin receptor was shown to be the optimal nNOS PDZ binding sequence[10,11]. Fig. 1*a* shows a stereo view of the best-fit superposition of a family of 15 structures of the complex. Due to the low content of aromatic amino acids within nNOS PDZ (three in total, Phe 21, Phe 30, and Tyr 77 in the hydrophobic core of the canonical PDZ domain), the 94 methyl groups of the protein displayed limited spectral resolution. Despite this inherent resonance degeneracy, we were able to determine the complex structure at a relatively high resolution by a combination of 2D homonuclear, and 3D/4D heteronuclear NMR spectroscopy (Fig. 1*a*, Table 1). The 4D $^{13}C/^{13}C$ NOESY was particularly useful in unambiguously assigning ^{13}C-separated NOE

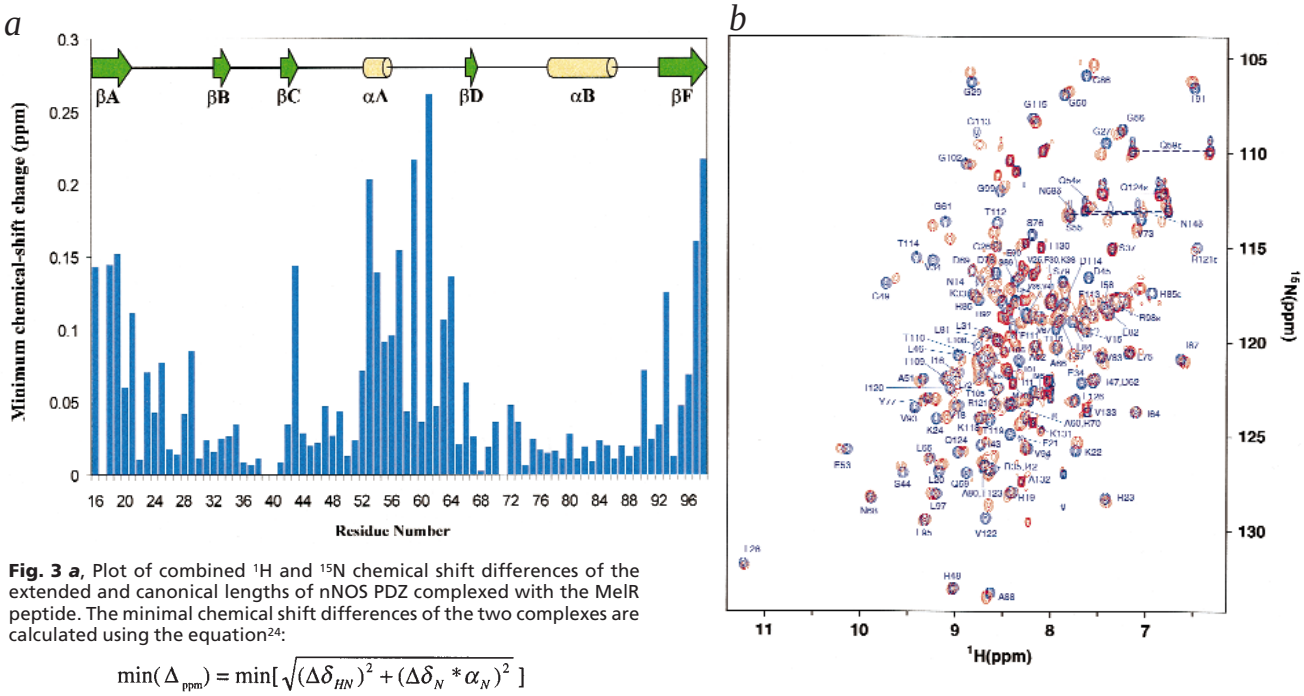

Fig. 3 ***a***, Plot of combined ^{1}H and ^{15}N chemical shift differences of the extended and canonical lengths of nNOS PDZ complexed with the MelR peptide. The minimal chemical shift differences of the two complexes are calculated using the equation[24]:

$$\min(\Delta_{ppm}) = \min[\sqrt{(\Delta\delta_{HN})^2 + (\Delta\delta_N * \alpha_N)^2}\,]$$

The scaling factor (α_N) used to normalize the ^{1}H and ^{15}N chemical shifts is 0.17. The chemical shift differences for the Pro residues are not plotted. For comparison, the secondary structure of the protein is shown above the plot. ***b***, The overlay plot of the ^{1}H-^{15}N HSQC spectra of nNOS PDZ complexed with the MelR peptide (blue) and the CAPON peptide (red). The assignment of the nNOS PDZ–MelR peptide complex is labeled with individual amino acid name and residue number.

crosspeaks[22]. The nNOS PDZ domain contains a core of five β-strands (βA–F) and two α-helices (A and B) (Fig. 1*c*). Two additional β-strands (β'I and β'II) at the C-terminus pack loosely with the core of nNOS PDZ. As predicted by the amino acid sequence, the residues 14–98 form a compact PDZ domain structure having an overall topology similar to the other PDZ domains determined by X-ray crystallography and NMR spectroscopy (an r.m.s. difference of 1.91 Å when compared with the X-ray structure of the third PDZ domain of PSD-95 complexed with a four residue peptide using the secondary structure elements of the complexes)[7,14–16]. The MelR peptide binds to the pocket formed by βB and αB at an antiparallel β-strand structure (Fig. 1*c*). However, significant differences do exist in the loop regions, αA, and βD, when compared to the crystal structure of the PSD-95 PDZ–peptide complex[7]. In particular, the loop connecting αA and βD, as well as the orientation of αA are significantly different between the two structures. The differences likely arise from the packing of the C-terminal extension with these regions of nNOS PDZ. In addition, βD in nNOS PDZ is three residues shorter, and βE is not detected (Fig. 1*c*).

One of the most striking features of the nNOS PDZ–MelR peptide complex structure is the short antiparallel β-sheet (β'I of residues 103–106, and β'II of 122–125) C-terminal to the canonical PDZ domain (Fig. 1*c*). The side chains of Thr 104, Thr 105 from β'I and Thr 119 and Ile 120 prior to β'II make van der Waals interactions with the beginning of βA and the loop connecting αA and βD, resulting in the loose packing of the C-terminal extension with the core of the PDZ domain (Fig. 1*a*). The loop connecting β'I and β'II is flexible as indicated by NOE contacts and heteronuclear ^{1}H-^{15}N NOE values (data not shown; Fig. 1*a*). However, superposition of the 15 NMR structures using β'I and β'II showed that the C-terminal β-sheet is also well defined by itself (Fig. 1*b*; Table 1). Among numerous PDZ domains, the nNOS PDZ domain is the only one known to form dimers with the corresponding PDZ domains from α-syntrophin and PSD-95/PSD-93[9]. The C-terminal extension was shown to be absolutely required for such PDZ dimer formation[9,10]. It was further demonstrated that the binding sites within the PDZ domain of PSD-95 for Thr/Ser-X-Val* peptides and nNOS PDZ overlap with each other[9]. These data suggest that the C-terminal extension of nNOS PDZ binds to the Thr/Ser-X-Val* peptide binding groove of the PDZ domain of PSD-95. It was previously proposed that not only C-terminal peptides but also internal β-strands might interact with PDZ domains[4]. Indeed, it was shown that the PDZ domain of α-syntrophin was able to bind to a restrained cyclic peptide with high affinity[23]. Formation of complexes with internal peptide fragments from their respective targets may be another general mode of interaction for many PDZ domains[12,13]. Taken together, it is very likely that one of the internal β-strands in the C-terminal extension of nNOS PDZ binds to the target recognition groove in the PDZ domains of α-syntrophin and PSD-95. Once forming complexes with α-syntrophin or PSD-95, the loosely packed C-terminal extension may detach from the rest of the domain. Experiments are currently in progress to elucidate the exact amino acid sequence of nNOS PDZ that mediates the interaction with the PDZ domain of PSD-95.

Peptide-binding pocket

Similar to the class I PDZ domains, nNOS PDZ has a conserved 'GLGF' carboxylate-binding motif (Fig. 2*a*,*c*)[7,8]. As expected, the hydrogen bonding pattern between the -COOH of the MelR peptide and the backbone amides of the 'GLGF' motif is similar to that observed in the previously determined PDZ–peptide complex structures[7,15,16] (Fig. 2*a*). The side chain of Val 0 is situated deep in a hydrophobic pocket comprised of the highly conserved hydrophobic amino acids of Leu 28, Phe 30 and Leu 84 (Fig. 2*b*,*c*). Two additional hydrophobic residues (Ile 87 and Val 94) located at the perimeter of the pocket also partially interact with the side chain of Val 0 in the peptide (Fig. 2*a*).

The nNOS PDZ domain has a strong preference for negatively

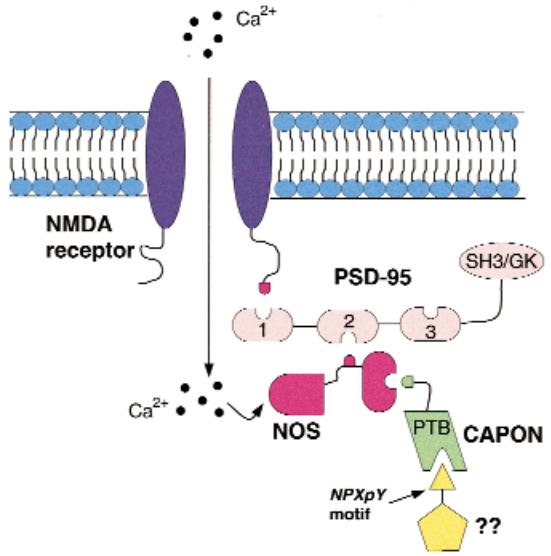

Fig. 4 Model for nNOS signal transduction complex organization by PDZ domains. The NMDA receptors are clustered by multiple PDZ domain containing PSD-95. The multimeric PSD-95 further couples nNOS to the NMDA receptors, allowing direct activation of nNOS by influxes of Ca^{2+}. The PDZ domain of nNOS can further recruit its binding protein such as CAPON by binding to its C-terminal tail. The PTB domain of CAPON may bind to as yet unknown NPXpY motif containing proteins in the signaling pathway.

charged amino acids at the –2 position of its peptide ligands[10,11]. Therefore, nNOS PDZ represents a novel class (class III) PDZ domain (Fig. 2*c*). The selectivity at the –2 position of peptide ligands by various PDZ domains is largely determined by the amino acid residue in αB1[7,8]. In the case of nNOS PDZ, the hydroxyl group of Tyr 77 in αB1 forms a hydrogen bond with the carboxyl group of Asp –2 of the ligand (Fig. 2*a*). Oriented peptide library studies showed that a PDZ domain containing an Asp in place of Tyr at αB1 selectively binds to peptide ligands with Tyr at the –2 position, thus supporting the selectivity of Tyr and Asp/Glu at the two positions against each other[8]. The selectivity of nNOS PDZ for a negatively charged amino acid residue at the –2 position is also contributed by the positively charged Arg 85 side chain of the protein (Fig. 2*a*,*b*). In class I PDZ, the αB1 is a His residue and it selects for Ser or Thr at the –2 position by forming a hydrogen bond between the hydroxyl group of Ser/Thr and Nε of His[7,8]. Mutation of Tyr 77 to His in nNOS PDZ changes the ligand binding specificity from Asp-X-Val* to Ser/Thr-X-Val*[11]. The presence of a hydrophobic residue (class II) at αB1 predestines these PDZ domains to selectively bind to C-terminal peptides with hydrophobic amino acids in the –2 position[8,16].

Effect of the C-terminal truncation

While it is certain that the C-terminal extension is required for nNOS PDZ to interact with the PDZ domains from α-syntrophin and PSD-95, it remains open to debate whether the same extension is essential for the domain to interact with C-terminal peptides[10,11,20]. To resolve this issue, we studied the interactions of the MelR peptide with nNOS PDZ with and without the C-terminal extension by comparing the ^{1}H-^{15}N HSQC spectra of the two forms of the PDZ domain complexed with the MelR peptide. Chemical shift differences between the two complexes using the minimal shift difference approach[24] are shown (Fig. 3*a*). Very little chemical shift differences are observed in the peptide binding pockets and its peripheral regions between the two complexes, indicating that peptide binding is unlikely to be affected by the C-terminal extension. The regions that show large chemical shift differences are the areas with which the C-terminal extension interacts (Figs 1*c*, 3*a*). This is expected since the shift perturbation is a direct result of the deletion of the extension. We have also studied the binding of the biotinylated MelR peptide with the two forms of nNOS PDZ using surface plasmon resonance. The data suggest that the MelR peptide binds to the PDZ domain of both forms in an indistinguishable manner (data not shown). These results can be readily explained by the three dimensional structure of the complex (Fig. 1). The C-terminal extension and the peptide binding groove are located at the two opposite sides of the PDZ domain and no contacts are observed between the residues in the two regions of the protein. Therefore, we conclude that the canonical nNOS PDZ domain (residues 11–98) is sufficient for its binding to C-terminal Asp-X-Val* peptides.

Interaction with the CAPON peptide

It has been suggested that CAPON may regulate cellular nNOS activity by altering its localization from the membrane to the cytosol[20]. Unexpectedly, CAPON has a C-terminal sequence different from the previously identified Asp-X-Val* motif. Similar to the finding described here, the canonical nNOS PDZ domain is sufficient for CAPON interaction[20]. We asked whether the Asp-X-Val* peptide and the C-terminus of CAPON bind to the same site on nNOS PDZ. To address this issue, a peptide corresponding to the last 12 amino acid residues of CAPON (ELGDSLDDEIAV) was synthesized to study its interaction with nNOS PDZ. The overlay plot of the ^{1}H-^{15}N HSQC spectra of nNOS PDZ complexed with MelR peptide (*blue*) and the CAPON peptide (*red*) is shown (Fig. 3*b*). The two spectra are strikingly similar, and the resonances corresponding to the residues in the peptide binding groove of the two PDZ complexes are nearly superimposable, indicating that the two peptides binding sites in nNOS PDZ overlap with each other. Moreover, NMR titration experiments also showed that the two peptides compete with each other in binding to nNOS PDZ (data not shown). These data, together with the structure (Fig. 1), suggest that CAPON is unlikely to compete with PSD-95 for nNOS[20]. Indeed, it has been independently shown that a similar CAPON peptide does not block the association between the long nNOS PDZ domain and the PDZ domain of PSD-95 (David Bredt, personal communication).

The structural and biochemical data from this work together with previous findings suggest the following model (Fig. 4). The C-terminal tail of an N-methyl-D-aspartate (NMDA) receptor binds to one of the PDZ domains of PSD-95. Organization of nNOS into the NMDA receptor–PSD-95 complex is mediated by the binding of the C-terminal extension in nNOS PDZ to the second PDZ domain of PSD-95. The nNOS PDZ domain can further interact with related proteins such as CAPON using its PDZ domain. It is possible that the phosphotyrosine binding (PTB) domain of CAPON may further recruit as yet unknown Asn-Pro-Xaa-pTyr motif containing proteins[4,20]. The model proposed here presents another example showing the role of PDZ domains as versatile scaffolds in organizing signal transduction complexes[5].

Methods

Sample preparations. The long rat nNOS PDZ domain (residues 11–133) was PCR amplified from rat brain cDNA and inserted into the plasmid pET14b (Novagen). The His-tagged nNOS PDZ domain was expressed in *Escherichia coli* BL21(DE3) cells. Uniformly ^{15}N-, and $^{15}N/^{13}C$-labeled nNOS PDZ samples were prepared as described[25]. The

Table 1 Structural statistics for the family of 15 structures[1]

Distance restraints	
Intraresidue (i-j = 0)	577
Sequential (li-jl = 1)	421
Medium range (2 ≤ li-jl ≤ 4)	196
Long range (li-jl ≥ 5)	442
Hydrogen bonds	44
Intermolecular	54
Total	1,734
Dihedral angle restraints	
Φ	46
Ψ	45
Total	91
Mean r.m.s. deviations from the experimental restraints	
Distance (Å)	0.033 ± 0.001
Dihedral angle (°)	0.81 ± 0.11
Mean r.m.s. deviations from idealized covalent geometry	
Bond (Å)	0.004 ± 0.000
Angle (°)	0.56 ± 0.02
Improper (°)	0.40 ± 0.02
Mean energies (kcal mol $^{-1}$)	
E_{NOE}[2]	97.3 ± 7.1
E_{cdih}[2]	3.72 ± 1.04
E_{repel}	118.4 ± 10.4
E_{L-J}	–344.9 ± 12.0
Ramachandran plot[3]	
Residues 15–98	
% Residues in the most favorable regions	63.4
Additional allowed regions	35.4
Generously allowed regions	0.9
Atomic r.m.s. differences (Å)[4]	
Residues 15–98 in protein and –3 to 0 in peptide	
Backbone heavy atoms (N, Cα, C' and O)	0.48
Heavy atoms	0.90
Residues 15–34, 41–98 in protein and –3 to 0 in peptide	
Backbone heavy atoms (N, Cα, C' and O)	0.43
Heavy atoms	0.79
Residues 98–100 (β'I) and 116–118 (β'II)	
Backbone heavy atoms (N, Cα, C' and O)	0.41
Heavy atoms	0.84

[1]None of the structures exhibits distance violations greater than 0.3 Å or dihedral angle violations greater than 5°.
[2]The final values of the square-well NOE and dihedral angle potentials were calculated with force constants of 50 kcal mol^{-1} Å $^{-1}$ and 200 kcal mol^{-1}rad^{-1}, respectively.
[3]The program PROCHECK[36] was used to assess the overall quality of the structures.
[4]The precision of the atomic coordinates is defined as the average r.m.s. difference between the 15 final structures and the mean coordinates of the protein.

His-tagged nNOS PDZ domain purified from a Ni^{2+}-NTA column was digested with thrombin, and the His-tag was removed by gel filtration chromatography. The C-terminal truncated form of nNOS PDZ (residues 11–98) were prepared using the identical method described for the long form of the PDZ domain. The synthetic peptides used were commercially obtained. NMR samples were dissolved in 100 mM potassium phosphate buffer at pH 6.0. The concentrations of the samples were in the range of 1.0–1.4 mM. Due to the low solubility of free nNOS PDZ it was not possible to obtain interpretable NMR spectra.

NMR spectroscopy. All NMR spectra were recorded at 35 °C on a Varian Inova 500 spectrometer equipped with an actively *z*-gradient shielded triple resonance probe. Sequential backbone and side chain assignments of the nNOS PDZ in the complex were obtained using standard heteronuclear multidimensional NMR experiments[26]. Stereospecific assignment of the methyl groups of Val and Leu was achieved using a 10% ^{13}C-labeled sample[27]. The backbone coupling constants ($^3J_{NH\alpha}$) of nNOS PDZ were measured as described[28].

Structure calculations. Approximate interproton distances were obtained from four NOESY spectra (a 3D ^{15}N-separated, a 3D ^{13}C-separated, a 4D ^{13}C/^{13}C-separated, and a homonuclear ^{1}H 2D NOESY experiments, see ref. 25 for details). The intermolecular NOEs between the labeled PDZ domain and the unlabeled peptide were obtained by a 3D ^{13}C F_1-filtered, F_3-edited NOESY-HSQC[29]. The distance and dihedral angle restraints were classified as described previously[25]. Hydrogen bond restraints were generated from the standard secondary structures of the protein based on the NOE patterns. The NMR structures were calculated using a standard distance geometry/simulated annealing protocol[30] using the program X-PLOR[31].

Illustrations. The figures were prepared using the programs MOLMOL[32], MOLSCRIPT[33], Raster3D[34], and GRASP[35].

Coordinates. The coordinates of the structures for the nNOS PDZ–MelR complex have been deposited in the Protein Data Bank (accession code 1B8Q).

Acknowledgments

We thank L. E. Kay for providing NMR pulse sequences, R. Muhandiram for help with the NMR experiments, D. Bredt for communicating unpublished experimental results, and D. Miller-Martini for critical reading and comments on the manuscript. This research was supported by the RGC grants from the Research Grant Council of Hong Kong. The NMR spectrometer used in this work was purchased by the Biotechnology Research Institute of HKUST.

Correspondence should be addressed to M.Z. *email: mzhang@uxmail.ust.hk*

Received 3 February, 1999; accepted 8 March, 1999.

1. Ponting, C.P., Phillips, C., Davies, K.E. & Blakes, D.J. *BioEssays* **19**, 469–479 (1997).
2. Sheng, M. *Neuron* **17**, 575–578 (1996).
3. Craven, S.E. & Bredt, D.E. *Cell* **93**, 495–498 (1998).
4. Harrision, S.C. *Cell* **86**, 341–343 (1996).
5. Tsunoda, S. *et al. Nature* **388**, 243–249 (1997).
6. Kaech, S.M., Whitfield, C.W. & Kim, S.K. *Cell* **94**, 761–771 (1998).
7. Doyle, D.A. *et al. Cell* **85**, 1067–1076 (1996).
8. Songyang, Z. *et al. Science* **275**, 73–77 (1997).
9. Brenman, J.E. *et al. Cell* **84**, 757–767 (1996).
10. Schepens, J., Cuppen, E., Wiernga, B. & Hendriks, W. *FEBS Lett.* **409**, 53–56 (1997).
11. Stricker, N.L. *et al. Nature Biotech.* **15**, 336–342 (1997).
12. Shieh, B.H. & Zhu, M.Y. *Neuron* **16**, 991–998 (1996).
13. Cuppen, E., Gerrits, H., Pepers, B., Wieringa, B. & Hendriks, W. *Mol. Biol. Cell* **9**, 671–683 (1998).
14. Cabral, J.H.M. *et al. Nature* **382**, 649–652 (1996).
15. Schultz, L. *et al. Nature Struct. Biol.* **5**, 19–24 (1998).
16. Daniels, D.L., Cohen, A.R., Anderson, J.M. & Brüger, A.T. *Nature Struct. Biol.* **5**, 317–325 (1998).
17. Stuehr, D.J. *Annu. Rev. Pharmacol. Toxicol.* **37**, 339–359 (1997).
18. Jaffrey, S.R. & Snyder S.H. *Science* **274**, 774–777 (1996).
19. Fan, J.-S. *et al. J. Biol. Chem.* **273**, 33472–33481 (1998).
20. Jaffrey, S.R., Snowman, A.M., Eliasson, M.J., Cohen, N.A. & Snyder S.H. *Neuron* **20**, 115–124 (1998).
21. Vesely, D.L. *Mol. Cell Biochem.* **35**, 55–58 (1981).
22. Vuister, G.W. *et al. J. Magn. Reson.* **B101**, 210–213 (1993).
23. Gee, S.H. *et al. J. Biol. Chem.* **273**, 21980–21987 (1998).
24. Farmer, B.T. et al. *Nature Struct. Biol.* **3**, 995–997 (1996).
25. Tochio, H., Ohki, S., Zhang. Q., Li, M. & Zhang, M. *Nature Struct. Biol.* **5**, 965–969 (1998).
26. Bax, A. & Grzesiek, S. *Acc. Chem. Res.* **26**, 131–138 (1993).
27. Neri, D., Szyperski, T., Otting, G., Senn, H., & Wuthrich, K. *Biochemistry* **28**, 7510–7516 (1989).
28. Kay, L.E. & Bax, A. *J. Magn. Res.* **86**, 110–126 (1990).
29. Zwahlen, C. *et al. J. Am. Chem. Soc.* **119**, 6711–6721 (1997).
30. Nilges, M., Clore, G.M. & Gronenborn, A.M. *FEBS Lett.* **239**, 129–136 (1988).
31. Brüger, A.T. *X-PLOR. A system for X-ray crystallography and NMR* (Yale University Press, New Haven, Conneticut; 1992).
32. Koradi, R., Billeter, M. & Wuthrich, K. *J. Mol. Graph.* **14**, 51–55 (1996).
33. Kraulis, P.J. *J. Appl. Crystallogr.* **24**, 946–950 (1991).
34. Merritt, E. & Murphy, M. *Acta Cryst.* **D50**, 869–873 (1994).
35. Nicholls, A. *GRASP: graphical representation and analysis of surface properties* (Columbia University, New York, 1992).
36. Laskwoski, R.A., MacArthur, M.W., Moss, D.S. and Thornton, J.M. *J. Appl. Crystallogr.* **26**, 283–291 (1993).